Online Gait Optimization for Running in Resistive Media

Jason White[1], Max Austin[1], Jonathan Clark[1], Christian Hubicki[1], and Jason Pusey[2]

***Abstract*— In-field legged robots need gaits and behaviors that allow them to run over and through all types of terrain, including through fluidic media such as ponds, bogs, and sand dunes. This paper presents a method of rapidly generating legged running gaits, on-the-fly, for these resistive fluid-like terrains. To accelerate gait computation, we adapted a reduced-order dynamic model of legs in fluid fields for rapid optimization of energy-efficient motion plans. For the first time, we achieve online optimization for a legged model in resistive fluid-like media by formulating an optimal control problem with smooth and analytical cost functions and constraints. In numerical tests, we benchmark the computation times for our nonlinear optimization and validate that the optimized gaits follow a U-shaped speed versus cost curve commonly associated with energy optimal legged locomotion. We further present a proof-of-concept demonstration of optimized gaits on a planarized monopod robot hopping through a bed of fluidized granular material – a surrogate fluid-like substrate.**

***Keywords*—legged locomotion, running, optimal control, motion planning, rheology**

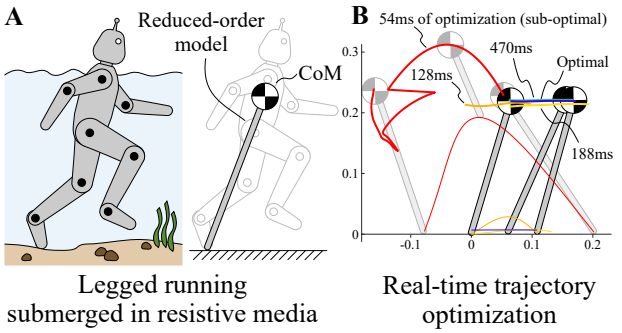

Fig. 1: This paper presents rapid optimization of legged locomotion in resistive media (e.g. fluids) A. An illustration of how a multi-body legged robot is abstracted to a reduced-order FF-SLIP model. B. The Cartesian CoM and foot trajectories of a gait during optimization, achieving near-optimal behavior in 470ms.

I. Introduction

Animals can run and bound through flowing, granular, and deformable substrates such as sand, tall grass, water, and mud. Further, animals can adapt their gaits to fit the substrate in a manner that seemingly optimizes for speed or energy consumption. We want controllers for legged robotic systems that synthesize gaits through these terrains, which we lump together under the term "resistive media." This paper extends state-of-the-art running control methods to include a computationally tractable fluid dynamic model to generate efficient locomotion through resistive media (Fig. 1A). We modify existing fluid dynamic models for legged locomotion to be both smooth and analytically differentiable, which allows us to generate running gaits in resistive media with a fast-solving optimization (< 2 seconds).

Running robot control dates back to tuned heuristics from the 1980's [1], but modern methods use model-based optimization to synthesize behaviors. While system models can be detailed with multibody dynamics [2], [3], reduced-order models can synthesize a variety of behaviors using simpler and faster computations [4], [5]. The Spring Loaded Inverted Pendulum (SLIP) model is a widely-used reduced-order model for running, reducing complexity by assuming a point-mass body and a massless linear spring leg [6]. The SLIP model is credited with inspiring successful leg control schemes [7], [8], but it is energetically passive and thus needs extension to control behaviors with changing mechanical energy. Actuated variants of SLIP models can use continuous-time inputs to stabilize running behaviors across energy levels–even in rough terrain [9], [10].

Running in a resisting force field complicates the locomotion plant model and thus further challenges control. Fluids, granular materials (sand), foliage, and colloids (mud), are all governed by different physical phenomena that are principally modeled by expensive calculations (Navier-Stokes, discrete element methods, continuum mechanics, and multi-physics solvers, respectively). Approaches for tractable resistive modeling, such as the U-SLIP model [11] (or Underwater SLIP), took a lumped modeling approach for synthesizing SLIP model gaits in a resistive media generating underwater "punting" gaits [12]. While the U-SLIP model ignored resistive forces on the leg, a subsequent approach modeled leg drag and generated gaits through different fluid depths [13]. This model used a black-box particle swarm optimization to find gaits in > 10 minutes. More recently, this model was extended to include buoyancy and drag on the body and leg called the Fluid-Field SLIP (FF-SLIP) model, and used a Newton-Raphson search to identify gait parameters [14]. This method of trajectory generation accommodates a more complex dynamic model but requires some gait parameters to be determined a priori (i.e. duty cycle, phase velocity conditions, etc.) to converge and again results in solve times on the order of minutes.

This paper details our approach toward generating running gaits online in resistive media in the following order. First, we detail the reduced-order fluid-field SLIP model [14] and present new modifications to its resistive media model to incorporate smooth analytical derivatives. Using direct tran-

[1] Florida A&M University-Florida State University, Tallahassee, FL
[2] DEVCOM Army Research Laboratory, Adelphi, MD

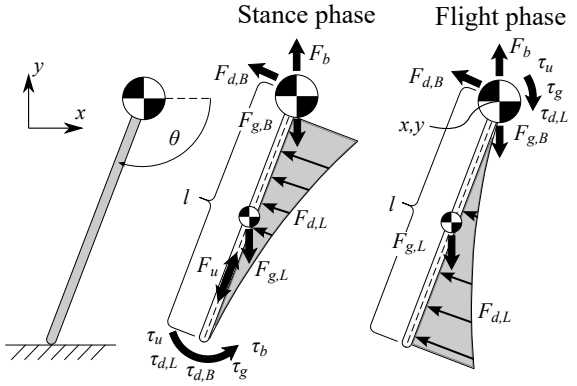

Fig. 2: Diagram of the presented reduced-order legged model in stance (foot contact) and flight (no foot contact) phases.

scription methods, we formulate this optimal control problem as a nonlinear program (NLP) and demonstrate that the smooth and easy-to-compute derivatives enable fast computation times (< 2 seconds). When systematically commanding a range of desired gait speeds, the optimization finds a trade-off with energy cost that is smooth and U-shaped - a well-established feature of locomotion in robotics [15] suggesting that the optimization is successfully minimizing energy waste. As a final proof of concept, we implement an example optimized gait (Fig. 1B) on a monopod robot immersed in aerated granular media (a dry substitute for flowing liquids) to demonstrate stable hopping through resistive media with these fast-synthesized gaits (Fig. 5C).

II. Methods

Here we present a method of online gait optimization for SLIP models in resistive media–the FF-SLIP. Optimal gaits minimize the cost of transport based on motor effort by translating the reduced order SLIP torques (τ_u) and forces (F_u) to motor torques (τ_M) for a five-bar Minitaur leg. Smooth analytical derivatives allow us to quickly optimize gaits via large-scale direct collocation despite our nonlinear equations of motion.

A. Conventions

Sub-scripted capital letters refer to forces applied to either the body (F_B) or the leg (F_L). Lower case subscripts indicate the source of force (F) or torque (τ), with the options being buoyancy (b), gravity (g), drag (d), and control input (u). A (k) subscript indicates an individual node in the optimization. Superscripts indicate flight (q^F) or stance (q^S). The system has four degrees of freedom; leg angle (θ), leg length (l), and Cartesian body position (x, y), with state vector (q) defined as

$$q = \begin{bmatrix} p & v \end{bmatrix}^T, \quad p = \begin{bmatrix} \theta & l & x & y \end{bmatrix}^T, \quad v = \dot{p}.$$

B. Dynamics

The presented method models both a single-legged robot and environmental forces using reduced-order dynamical approximations. Here, we derive a fluid-field forcing model that acts upon an actuated Spring-loaded Inverted Pendulum (SLIP) model. While the approximation makes several simplifying assumptions similar to [14], this reformulation novelly offers smooth analytical derivatives by assuming the system is fully submerged–thereby enabling fast online gait optimizations. Hopping/running requires changing contact modes, which we model independently as a stance (foot contact) phase and a flight (no foot contact) phase.

1) Stance phase: During stance, we assume the model has two degrees of freedom, leg rotation and telescoping extension, and lump the body mass and leg mass together into a single rigid mass. The foot is pinned to the ground by a revolute joint and leg extension is modeled by a prismatic joint (Fig. 2). We assign polar coordinates to these degrees of freedom, a leg angle (θ) w.r.t. the horizontal plane and a telescoping leg length (l). Control inputs during stance include a body torque (τ_u) and leg extension force (F_u), which when combined with F_g and torque τ_g generated by gravity, we find:

$$\begin{aligned} F_g &= -\underbrace{m_B g}_{F_{g,B}} - \underbrace{m_L g}_{F_{g,L}} \\ \tau_g &= -gl(m_B + \frac{m_L}{2})\cos(\theta) \end{aligned} \tag{1}$$

where m_B and m_L are the body and leg masses respectively. We compute upward buoyant forces from the displaced weight of the fluid of density, ρ,

$$\begin{aligned} F_b &= \rho V_B g \\ \tau_b &= \rho V_B g l \cos(\theta). \end{aligned} \tag{2}$$

The FF-SLIP model drag on the system from the resistive media (the same method used here) results in a single force on the body, and two torques about the toe:

$$\begin{aligned} F_{d,B} &= -\frac{\rho C_B A_B \dot{l}|\dot{l}|}{2} \\ \tau_{d,L} &= -\frac{\rho C_L W_L \dot{\theta}|\dot{\theta}|l^4}{8} \\ \tau_{d,B} &= -\frac{\rho C_B A_B \dot{\theta}|\dot{\theta}|l^3}{2} \end{aligned} \tag{3}$$

where the body drag force, $F_{d,B}$, and drag torques, $\tau_{d,L}$ and $\tau_{d,B}$, are dependent on the system velocity. We note the leg actuation F_u does not experience drag because the drag force is always normal to the leg.

Incorporating these forces into the equations of motion with a torsional and linear actuation force results in the following equations of motion

$$\begin{aligned} (m_B + m_L)\ddot{l} &= F_u + F_{d,B} - F_g \sin\theta - F_b \sin\theta \\ (m_B + \frac{m_L}{3})l^2\ddot{\theta} &= \tau_u + \tau_{d,B} + \tau_{d,L} - \tau_g - \tau_b. \end{aligned} \tag{4}$$

2) Flight phase: While not in ground contact, we redefine our coordinates in a Cartesian frame with x and y position coordinates. Additionally, we no longer consider the forces acting along the leg actuation direction because the telescoping length does not produce a force on the body in flight.

Simulated Leg Parameters			
Parameter	Symbol	Value	Units
Body mass	m_B	1.36	kg
Leg mass	m_L	0.19	kg
Leg Thickness	W_L	0.0512	m
Body Volume	V_B	0.0002	m^3
Body Area	A_B	0.007	m^2
Environmental/Geometric Parameters			
Gravitational Acceleration	g	9.81	m/s^2
Media Density	ρ	997	kg/m^3
Body Drag Coefficient	C_B	0.47	-
Leg Drag Coefficient	C_L	1.15	-

TABLE I: Fluid-field SLIP model (FF-SLIP) parameters

With our new reference frame the gravitation force remains the same, but the torque becomes

$$\tau_g = \frac{m_L g l \cos(\theta)}{2}. \tag{5}$$

Similarly, the buoyancy force (F_b) remains unchanged and buoyancy torque (τ_b) is eliminated. Using a moving reference frame (the body Cartesian position) makes finding the drag forces and torques more challenging. The drag forces experienced by the system are based on the velocity of the system. In stance we were able to assume the drag force was normal to the leg, however we now have a moving reference frame and this assumption no longer holds true. We instead find the velocity of the body CoM, v_L, as per:

$$v_L = \dot{y}\cos\theta - \dot{x}\sin\theta, \tag{6}$$

and use this to find the drag along the leg's length. Using this in conjunction with the body velocities $\dot{x}$ and $\dot{y}$ we find the directional drag forces and torques:

$$\begin{aligned} F_{d,B_x} &= -\frac{\rho C_B A_B \dot{x}|\dot{x}|}{2}, \quad F_{d,B_y} = -\frac{\rho C_B A_B \dot{y}|\dot{y}|}{2} \\ F_{d,L} &= -\frac{\rho C_L W_L l(\dot{\theta}|\dot{\theta}|l^2 + 3\dot{\theta}v_L l + 3v_L|v_L|)}{6} \\ \tau_{d,L} &= -\frac{\rho C_L W_L l^2(3\dot{\theta}|\dot{\theta}|l^2 + 8\dot{\theta}v_L l + 6v_L|v_L|)}{24}. \end{aligned} \tag{7}$$

Incorporating these forces with the torsional actuation force results in the following equations of motion:

$$\begin{aligned} (m_B + \frac{m_L}{3})l^2\ddot{\theta} &= \tau_u + \tau_{d,L} - \tau_g \\ (m_B + m_L)\ddot{x} &= F_{d,B_x} - F_{d,L}\sin\theta \\ (m_B + m_L)\ddot{y} &= F_{d,B_y} + F_{d,L}\cos\theta + F_g + F_b. \end{aligned}$$

C. Assumptions

While the optimization methods can be broadly applied to running in resistive media generally, our presentation specifically uses kinematic and dynamic model parameters that match our testbed platform, the Minitaur leg (Fig. 5B). The model assumes buoyancy generates little to no force or torque on the system, and is therefore excluded. Contrary to the FF-SLIP model seen in [14], we assume the entire leg length is submerged. This assumption allows us to remove the surface swimming equilibrium factor, and eliminates discontinuities in the dynamics associated with the leg being exposed to multiple substrates (*i.e.* air and water) at the same time. We were also able to mathematically resolve the integral based fluid drag force used for distributed dynamic loads over the variable leg depth. Leg acceleration $\left(\ddot{l}\right)$ is defined during flight via a forced second-order model using an actuation force (F_u) and an added damping term (c) per:

$$m_L\ddot{l} = F_u - c\dot{l} - m_L g. \tag{8}$$

Drag forces heavily depend on the leg length, so allowing actuation during flight lets the optimization determine an optimal leg length to minimize the cost of transport. The damping term discourages unrealistic instantaneous changes in leg length. To smooth the absolute value terms for analytical differentiation, we use the approximation $\|z\| \approx \sqrt{z^2 + \varepsilon^2}$ where $\varepsilon \ll 1$.

D. Optimal Control Problem

The optimal control problem is cast as a nonlinear direct collocation trajectory optimization [16].

$$\begin{aligned} \min_{q,u,t} \quad & f(q,u,t) \\ \text{s.t.} \quad & c_1(q,u,t) = 0 \\ & c_2(q,u,t) \leq 0 \end{aligned} \tag{9}$$

where q is the system state vector $q_k = [p_k \; v_k]^T$ with $p_k = [\theta_k \; l_k \; x_k \; y_k]^T$, u is the control input vector $u_k = [F_{u,k} \; \tau_{u,k}]^T$, and t is the total phase duration. Each state and input is represented as a vector of N decision variables for $k \in \{1:N\}$. The equality ($c_1(q,u,t)$) and inequality ($c_2(q,u,t)$) constraints (detailed below) encode the system dynamics, continuity between modes, and task requirements. We then attempt to minimize the overall cost of transport in the cost function ($f(q,u,t)$) across both modes (stance and flight).

1) Dynamics Constraints: To enforce the system dynamics on the evolution of state variables, we add node-to-node defect constraints using Explicit Euler integration ($N = 101$ nodes per mode) with state derivatives per the previous section.

$$q_{k+1} = q_k + \dot{q}_k \Delta t, \quad \Delta t = \frac{t}{N-1}$$

The two separate modes are connected using continuity constraints.

2) Continuity Constraints: SLIP models inherently have discontinuous dynamics when switching from stance to flight. To address this, we create a mode schedule for the trajectory optimization, with the first mode being ground contact and the second having no ground contact. To enforce continuity at the interchange point, we use equality constraints to make the final mode 1 states equal to the initial mode 2 states. Enforcing gait periodicity is achieved in a similar manner, by constraining to the initial mode 1 states to equal the final mode 2 states,

$$\begin{aligned} 0 &= q^S_{final} - q^F_{init} \quad \text{(Mode continuity)} \\ 0 &= q^F_{final} - q^S_{init} \quad \text{(Periodicity)}. \end{aligned}$$

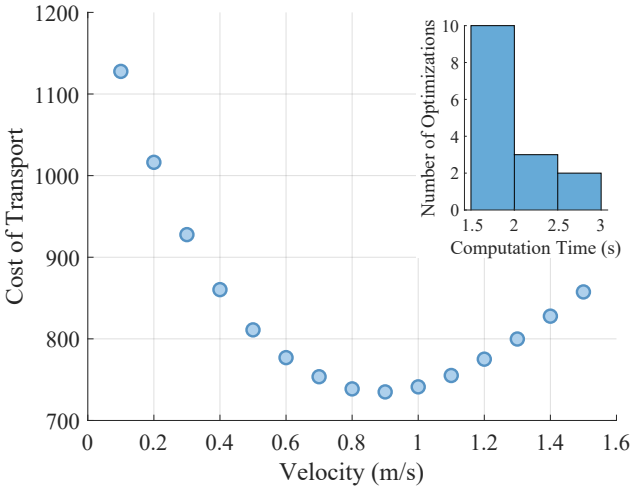

Fig. 3: Cost of transport and solve times for gaits of varied speeds. The COT curve is smooth and U-shaped – a common feature of energy-minimizing locomotion that suggests the optimization is avoiding pseudominima.

3) Kinematic Constraints: Additional constraints are added to limit the operating range of our system, and match kinematic limits using the 0.1m upper bar lengths (l_1) and 0.2m lower bar lengths (l_2) of the Minitaur testbed platform,

$$0.1 \leq l \leq 0.3 \qquad \text{(Leg length limit)}$$
$$-\frac{3\pi}{4} \leq \theta \leq -\frac{\pi}{4} \qquad \text{(Leg angle limit)}$$
$$0 \leq y + l\sin(\theta) \quad \text{(Toe above ground).}$$

4) Task Constraints: We add task constraints to prevent trivial zero-duration gaits (duration $> 0.001s$), and further prevent backward locomotion and allow only unilateral contact forces:

$$0.1 \leq x_{final} - x_{init} \qquad \text{(Forward motion)}$$
$$0 \leq F_l \qquad \text{(Unilateral leg force).}$$

5) Control Input Constraints: Limiting the control inputs to remain within our hardware limits is critical to successfully transitioning model-based control to a hardware platform. Motor torques are calculated via constraints that map the reduced-order FF-SLIP (Fig. 2) to a five-bar leg morphology (Fig. 4A) using a kinematic relationship. We use the law of cosines to find interior leg angles

$$\cos(\phi) = \frac{l_1^2 + l_2^2 - l^2}{2l_1 l_2}, \quad \cos(\psi) = \frac{l_2^2 + l^2 - l_1^2}{2l_2 l} \tag{10}$$

where ϕ is the angle between the virtual leg and the upper link, and ψ is the angle between the upper and lower leg links. Solving for ϕ requires a $\cos^{-1}$ term which frequently caused optimization infeasibility, so we introduce slack variables $s_1 = \cos(\phi)$ and $s_2 = \cos(\psi)$. Using equality constraints $s_1 - \cos(\phi) = 0$ and $s_2 - \cos(\psi) = 0$ allows us to reliably find optimal solutions. We then estimate the torques using

$$\tau_{M1} = \frac{F_u l_1}{2\cos\phi\sin\psi} + \frac{\tau_u}{2}, \quad \tau_{M2} = \frac{F_u l_1}{2\cos\phi\sin\psi} - \frac{\tau_u}{2} \tag{11}$$

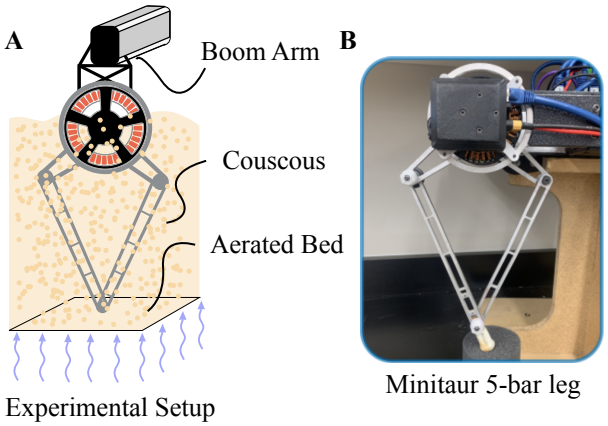

Fig. 4: A. Schematic of a two-motor five-bar monopod robot planarized by rigid attachment to a 2-DOF boom arm. Fluid resistance is emulated by an aerated bed of dry granular media (couscous). B. A five-bar "Minitaur" robot leg.

and limit these torques based on the T-Motor U10 KV100 maximum torque per:

$$|\tau_{M1}|,\ |\tau_{M2}| \leq 5.91. \tag{12}$$

Compared to torques computed with the Jacobian relation, $[\tau_{M1}\ \tau_{M1}]^T = J(l)[F_u\ \tau_u]^T$, the estimates are conservative.

6) Cost Function: As previously mentioned, we optimize for cost of transport (CoT) per:

$$\text{CoT} = \left(\int_0^t |\tau_{M1}| + |\tau_{M2}| dt\right) / (x_{final} - x_{init}). \tag{13}$$

We then export the NLP's costs, constraints, and their analytical derivatives using the MATLAB framework COALESCE [17]. We then solve the optimization using the open-source large-scale NLP solver, IPOPT [18].

III. Results

A. Numerical Results

Using the parameters seen in Table I, we generate trajectories which minimize the energetic cost of transport. We specify a target speed for each optimization by constraining the final velocity during flight. By generating optimal trajectories with increasing desired velocities by 0.1 m/s increments, we see the model's optimal running velocity occurs nearest to 0.9 m/s. Re-running the optimization without a prescribed velocity confirms the lowest-cost speed to be 0.887 m/s. The histogram included in this plot shows the majority of optimizations found the solution in under 2 seconds, demonstrating online computation speeds. One consistent feature of the optimized gaits is that almost no hip torque is required, which contrasts with previous FF-SLIP research finding actuating τ_u during swimming is optimal, producing a kick-back motion.

B. Hardware Results

We further test the model-based results by implementing the optimal CoT gait in a hardware hopping experiment. The monopod is a 2 DOF constrained Minitaur leg in an

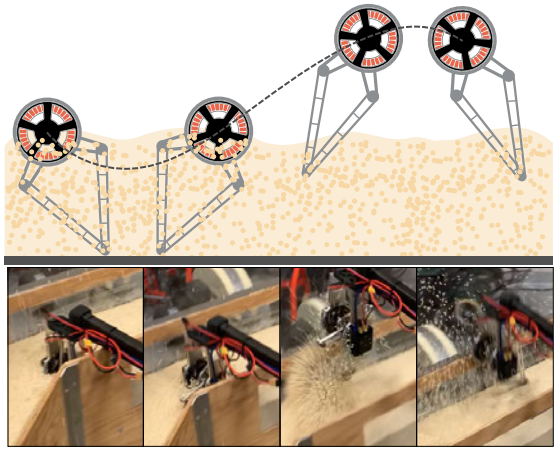

Fig. 5: Demonstration of fast-optimized monopod hopping through aerated couscous–a surrogate fluid-like substrate.

aerated couscous bed, as illustrated in (Fig. 5A), similar to [19]. This setup simulates a viscous fluid media without exposing the leg to normal risks associated with submerging electrical components in liquid. Our initial findings (after only a handful of tests) show additional constraints are needed in order to generate stable gaits. Although the optimal CoT gaits were able to move the leg through the media, the foot regularly slipped when in contact with the aerated bed. Additional constraints to enforce longer stance times and no instantaneous torques at touchdown/takeoff led to stable periodic motion of the leg resembling the gaits in simulation, as depicted in tiles in Fig. 5.

IV. Conclusion

We presented a framework for optimizing SLIP model trajectories through resistive media during operation ($\sim 1Hz$). Furthermore, we generated trajectories at different desired velocities, and tested the optimal cost of transport trajectory on a hardware platform. The results suggest that, with the presented parameters, there is a globally optimal gait minimizing cost of transport that can be found in under two seconds. Additionally, we show that the presented energy-efficient gaits are also stable when preliminarily tested on hardware with a robotic "Minitaur" leg.

Ongoing work will extend the formulation to include running with transitions between media (*e.g.* half in air and half in water). Using differentiable functions to represent fluid-air boundaries (*e.g.* sigmoids) will preserve the online optimization speeds while making the resistive drag forces from the media more precise. Measuring deviations between simulation and hardware will both 1) provide insight into the accuracy of our model and 2) allow the model to modify the drag coefficients via online regression. Taking advantage of the solve time, we aim to generate gaits on-the-fly to match these online-fitted models, enabling rapidly adaptive behaviors to new media *in situ*.

Acknowledgment

Authors JW, MA, JC, and CH are with the FAMU-FSU College of Engineering in Tallahassee, FL USA. Author JP is with the U.S. Army CCDC Army Research Laboratory in Adelphi, MD USA.

Research was sponsored by the DEVCOM Army Research Laboratory and was accomplished under Cooperative Agreement Number W911NF-16-2-0008. The views and conclusions contained in this document are those of the authors and should not be interpreted as representing the official policies, either expressed or implied, of the Army Research Laboratory or the U.S. Government. The U.S. Government is authorized to reproduce and distribute reprints for Government purposes notwithstanding any copyright notation herein.

References

[1] M. H. Raibert, *Legged robots that balance*. MIT press, 1986.

[2] K. Sreenath, H.-W. Park, I. Poulakakis, and J. W. Grizzle, "Embedding active force control within the compliant hybrid zero dynamics to achieve stable, fast running on mabel," *The International Journal of Robotics Research*, vol. 32, no. 3, pp. 324–345, 2013.

[3] A. Hereid, S. Kolathaya, and A. D. Ames, "Online optimal gait generation for bipedal walking robots using legendre pseudospectral optimization," in *2016 IEEE 55th Conference on Decision and Control (CDC)*. IEEE, 2016, pp. 6173–6179.

[4] C. Hubicki, A. Abate, P. Clary, S. Rezazadeh, M. Jones, A. Peekema, J. Van Why, R. Domres, A. Wu, W. Martin, H. Geyer, and J. Hurst, "Walking and running with passive compliance: Lessons from engineering: A live demonstration of the atrias biped," *IEEE Robotics Automation Magazine*, vol. 25, no. 3, pp. 23–39, 2018.

[5] J. Di Carlo, P. M. Wensing, B. Katz, G. Bledt, and S. Kim, "Dynamic locomotion in the mit cheetah 3 through convex model-predictive control," in *2018 IEEE/RSJ international conference on intelligent robots and systems (IROS)*. IEEE, 2018, pp. 1–9.

[6] W. J. Schwind, *Spring loaded inverted pendulum running: A plant model*. University of Michigan, 1998.

[7] A. Seyfarth, H. Geyer, M. Günther, and R. Blickhan, "A movement criterion for running," *Journal of biomechanics*, vol. 35, no. 5, pp. 649–655, 2002.

[8] M. Ernst, H. Geyer, and R. Blickhan, "Extension and customization of self-stability control in compliant legged systems," *Bioinspiration & biomimetics*, vol. 7, no. 4, p. 046002, 2012.

[9] B. Andrews, B. Miller, J. Schmitt, and J. E. Clark, "Running over unknown rough terrain with a one-legged planar robot," *Bioinspiration & biomimetics*, vol. 6, no. 2, p. 026009, 2011.

[10] G. Piovan and K. Byl, "Reachability-based control for the active slip model," *The International Journal of Robotics Research*, vol. 34, no. 3, pp. 270–287, 2015.

[11] M. Calisti and C. Laschi, "Underwater running on uneven terrain," in *OCEANS 2015-Genova*. IEEE, 2015, pp. 1–5.

[12] G. Picardi, C. Laschi, and M. Calisti, "Model-based open loop control of a multigait legged underwater robot," *Mechatronics*, vol. 55, pp. 162–170, 2018.

[13] R. Alicea, K. Ladyko, and J. Clark, "Lift your leg: Mechanics of running through fluids," in *2019 International Conference on Robotics and Automation (ICRA)*. IEEE, 2019, pp. 7455–7461.

[14] M. P. Austin and J. E. Clark, "The fluid field slip model: Terrestrial-aquatic dynamic legged locomotion," in *2021 IEEE International Conference on Robotics and Automation (ICRA)*. IEEE, 2021, pp. 4948–4954.

[15] W. Xi, Y. Yesilevskiy, and C. D. Remy, "Selecting gaits for economical locomotion of legged robots," *The International Journal of Robotics Research*, vol. 35, no. 9, pp. 1140–1154, 2016.

[16] O. V. Stryk, "Numerical solution of optimal control problems by direct collocation," in *Optimal control*. Springer, 1993, pp. 129–143.

[17] M. S. Jones, "Optimal control of an underactuated bipedal robot," 2014.

[18] L. T. Biegler and V. M. Zavala, "Large-scale nonlinear programming using ipopt: An integrating framework for enterprise-wide dynamic optimization," *Computers & Chemical Engineering*, vol. 33, no. 3, pp. 575–582, 2009.

[19] C. Li, T. Zhang, and D. I. Goldman, "A terradynamics of legged locomotion on granular media," *Science*, vol. 339, no. 6126, pp. 1408–1412, 2013.